THE EXTENDED STAR FORMATION HISTORY OF THE ANDROMEDA SPHEROID AT 35 KPC ON THE MINOR AXIS[1]

Thomas M. Brown[2], Rachael Beaton[3], Masashi Chiba[4], Henry C. Ferguson[2], Karoline M. Gilbert[5], Puragra Guhathakurta[5], Masanori Iye[6], Jasonjot S. Kalirai[5,7], Andreas Koch[8], Yutaka Komiyama[6], Steven R. Majewski[3], David B. Reitzel[8], Alvio Renzini[9], R. Michael Rich[8], Ed Smith[2], Allen V. Sweigart[10], Mikito Tanaka[6]
Accepted for publication in The Astrophysical Journal Letters

ABSTRACT

Using the *HST* ACS, we have obtained deep optical images reaching well below the oldest main sequence turnoff in fields on the southeast minor-axis of the Andromeda Galaxy, 35 kpc from the nucleus. These data probe the star formation history in the extended halo of Andromeda – that region beyond 30 kpc that appears both chemically and morphologically distinct from the metal-rich, highly-disturbed inner spheroid. The present data, together with our previous data for fields at 11 and 21 kpc, do not show a simple trend toward older ages and lower metallicities, as one might expect for populations further removed from the obvious disturbances of the inner spheroid. Specifically, the mean ages and [Fe/H] values at 11 kpc, 21 kpc, and 35 kpc are 9.7 Gyr and −0.65, 11.0 Gyr and −0.87, and 10.5 Gyr and −0.98, respectively. In the best-fit model of the 35 kpc population, one third of the stars are younger than 10 Gyr, while only ∼10% of the stars are truly ancient and metal-poor. The extended halo thus exhibits clear evidence of its hierarchical assembly, and the contribution from any classical halo formed via early monolithic collapse must be small.

Subject headings: galaxies: evolution – galaxies: stellar content – galaxies: halos – galaxies: individual (M31)

1. INTRODUCTION

One of the primary quests of astronomy is measuring the star formation history of giant galaxies. The most direct tool for such work is a color-magnitude diagram (CMD) reaching low-mass stars below the main sequence turnoff. The Advanced Camera for Surveys (ACS) on the *Hubble Space Telescope (HST)* enabled the application of this technique in the Andromeda Galaxy (M31), the nearest giant galaxy to our own. In a series of deep surveys, we have been exploring the star formation histories in M31's diverse structures (Brown et al. 2003, 2006, 2007).

The importance of M31 as a target for such studies is twofold. First, M31 is the only giant spiral galaxy where we can resolve the stellar main sequence with an external vantage point, thus overcoming the large uncertainties due to reddening and distance that can hamper studies of Milky Way field populations, most of which are too distant for accurate parallaxes. Second, recent studies suggest that M31 is more representative of large spiral galaxies than the Milky Way. By com-

paring their locations in the planes spanned by various parameters (rotational velocity, absolute K luminosity, disk angular momentum, [Fe/H] in the outskirts, disk scale length, etc.), Hammer et al. (2007) argue that M31 is more "typical" of large spirals than the Milky Way, which is systematically offset by ∼1σ from the dominant trends in these planes (see also Flynn et al. 2006). They attribute this distinction to an unusually quiescent merger history in the Milky Way. In contrast, the active merger history in M31 is supported by star count maps (e.g., Ferguson et al. 2002; Ibata et al. 2007) showing a variety of substructure, including a giant stellar stream (GSS) from a cannibalized satellite (Ibata et al. 2001).

Going back to the work of Mould & Kristian (1986), the M31 "halo" was considered unusual because of its relatively high metallicity (∼10 times higher than that in the Milky Way halo). Brown et al. (2003, 2006) have since demonstrated that these same metal-rich populations were of intermediate age (∼2–10 Gyr). There is now strong evidence that the inner spheroid (within 15 kpc) is polluted by the progenitor of the GSS; N-body simulations (Fardal et al. 2007) and kinematical surveys (Gilbert et al. 2007) demonstrate that much of the substructure in the inner spheroid is due to debris dispersed from the GSS's progenitor, while deep CMDs (Brown et al. 2006) show strong similarities between the star formation histories of the GSS and inner spheroid.

Recently, two groups independently discovered a vast extended halo in M31 (Guhathakurta et al. 2005; Irwin et al. 2005), spanning radii of 30–165 kpc and reaching lower metallicities similar to those in the Milky Way halo (Kalirai et al. 2006; Koch et al. 2007). Our purpose here is to measure the star formation history in this extended halo and to compare it to that in the interior fields. We have used the surface brightness profile of Guhathakurta et al. (2005) as a guide to this exploration (Figure 1). Brown et al. (2003, 2006) explored a field at 11 kpc on the minor axis, a metal-rich region of the spheroid that resembles a bulge, with significant debris from the merger that produced the GSS. Brown et al. (2007) investigated a field at 21 kpc, falling in the transition zone between

[1] Based on observations made with the NASA/ESA *Hubble Space Telescope*, obtained at STScI, and associated with proposal 10816.
[2] Space Telescope Science Institute, Baltimore, MD 21218; tbrown@stsci.edu, ferguson@stsci.edu, edsmith@stsci.edu
[3] Deptartment of Astronomy, University of Virginia, Charlottesville, VA 22904-4325; rlb9n@virginia.edu, srm4n@virginia.edu
[4] Astronomical Institute, Tohoku University, Sendai 980-8578, Japan; chiba@astr.tohoku.ac.jp
[5] University of California Observatories / Lick Observatory, University of California, Santa Cruz, CA 95064; kgilbert@ucolick.org, raja@ucolick.org, jkalirai@ucolick.org
[6] National Astronomical Observatory, Tokyo 181-8588, Japan; m.iye@nao.ac.jp, komiyama@subaru.naoj.org, mikito.tanaka@nao.ac.jp
[7] Hubble Fellow
[8] Department of Physics and Astronomy, University of California, Los Angeles, CA 90095; akoch@astro.ucla.edu; reitzel@astro.ucla.edu, rmr@astro.ucla.edu
[9] Osservatorio Astronomico, I-35122 Padova, Italy; alvio.renzini@oapd.inaf.it
[10] NASA Goddard Space Flight Center, Greenbelt, MD 20771; allen.v.sweigart@nasa.gov
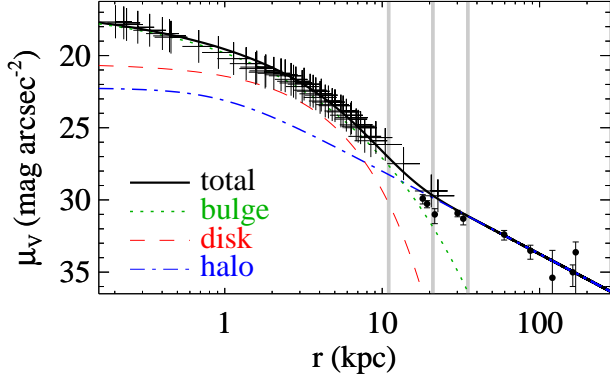
FIG. 1.— The minor-axis surface-brightness profile (*crosses*, Pritchet & van den Bergh 1994; *error bars*, Guhathakurta et al. 2005), along with one possible decomposition into disk, Sersic bulge, and $r^{-2.3}$ power-law halo (from Guhathakurta et al. 2005). A clear break in the surface-brightness profile occurs at 20–30 kpc. Our minor-axis fields (*grey shading*) sample the spheroid (i.e., bulge + halo) on either side of this transition region and within it.

the inner and outer spheroid. Here we investigate two fields at 35 kpc, where the extended halo begins to dominate.

2. OBSERVATIONS AND DATA REDUCTION

Using the ACS on the *HST* we obtained deep optical images of two minor-axis fields 2.6° (35 kpc) from the M31 nucleus, at $\alpha_{2000} = 00^h53^m28^s$, $\delta_{2000} = 39°49'46''$ and $\alpha_{2000} = 00^h54^m08^s$, $\delta_{2000} = 39°47'26''$. A third field was also in the observing queue when the ACS Wide Field Camera failed. The use of three fields was intended to provide a sample in the extended halo with at least as many stars as the single 21 kpc field in the transition zone. With only two fields, our 35 kpc sample is smaller than desired, but still sufficient to characterize the star formation history in the extended halo.

From Oct 2006 to Jan 2007, we obtained in each of our 35 kpc fields a total of 8 hours of images in the F606W filter (broad *V*) and 13 hours in the F814W filter (*I*). For one of these fields, two visits in the F814W filter failed due to guide star problems and were rescheduled with a 102° change in orientation. Every exposure was dithered to enable hot pixel removal, optimal point spread function (PSF) sampling, smoothing of spatial variation in detector response, and filling in the detector gap. Our reduction process is the same used by Brown et al. (2006) and only briefly summarized here. The images in a given field were registered, rectified, rescaled to $0.03''$ pixel^{-1}, and coadded using the DRIZZLE package (Fruchter & Hook 2002), with rejection of cosmic rays and hot pixels. PSF-fitting photometry, using the DAOPHOT-II software of Stetson (1987), was corrected to agree with aperture photometry of isolated stars, with the zeropoints calibrated at the 1% level. The final catalog with the photometry of both fields contains $\approx 8,500$ stars (Figure 2). Our photometry is in the STMAG system: $m = -2.5 \times \log_{10} f_\lambda - 21.1$. For those more familiar with the ABMAG system, ABMAG = STMAG -0.169 for m_{F606W}, and ABMAG = STMAG -0.840 mag for m_{F814W}. We performed extensive artificial star tests to characterize the photometric errors and completeness in the catalog. To avoid affecting the properties we were trying to measure, we added only 1000 artificial stars per pass, but by using thousands of passes, the tests contain over 8 million artificial stars.

Spectroscopic surveys (Gilbert et al. 2007; Koch et al. 2007) of red giant branch (RGB) stars in the M31 spheroid provide kinematical context for the ACS images. Figure 2 shows velocities from regions that include and surround the

ACS fields; for details on targeting, data reduction, velocity fitting, and separation of foreground dwarfs from M31 giants, see Gilbert et al. (2006) and Guhathakurta et al. (2006). Koch et al. (2007) obtain a similar velocity distribution at 35 kpc.

The CMD of our 35 kpc field is shallower and far less crowded than the CMDs of the inner spheroid, GSS, and outer disk obtained by Brown et al. (2006). Ideally, in our current program we would obtain the same depth and star counts, but the scarcity of stars in these fields forced us to investigate the trade-off between depth and star counts that could be achieved in a program of reasonable size. Through simulations, we found that we could determine the predominant star formation history even with one-tenth the number of stars and 0.2 mag less depth. The penalty is some loss of sensitivity to minority population components (e.g., few percent "bursts"), as demonstrated by Brown et al. (2007).

The images at 21 kpc and 35 kpc suffer from charge transfer inefficiency (CTI) in the ACS CCD due to radiation damage, but the 11 kpc images do not. The difference in CTI is due to the 4-year baseline between the 11 kpc field and the later fields, and also the higher stellar density in the 11 kpc field. As in Brown et al. (2007), we apply a CTI correction to our 35 kpc photometry. The correction is not applied to the artificial star tests, because artificial stars are not clocked across the detector. The correction makes the faint stars brighter, but it has a small effect on the star formation history fits (§3); without the correction, the 35 kpc population would appear to be 130 Myr older and 0.11 dex more metal-poor.

3. ANALYSIS

In Figure 2 we compare the spheroid populations at 11 kpc, 21 kpc, and 35 kpc, focusing on kinematics (*panels a–c*), CMDs (*panels d–f*), and star formation history fits (*panels g–i*). Each field hosts stars with a broad velocity distribution, centered on the M31 systematic velocity. None of the fields shows clear evidence of a dominant, kinematically-cold component, as might be expected if there were a majority contribution from a single stream or from the disk.

From CMD fitting, Brown et al. (2007) found the population at 21 kpc to have a mean metallicity that is 0.2 dex lower and a mean age that is 1.3 Gyr older than the population at 11 kpc. Those findings were confirmed by visual inspection of the CMDs. Compared to the 11 kpc population, the RGB ridge line of the 21 kpc population is 0.016 mag bluer, the fraction of horizontal branch (HB) stars blueward of the RR Lyrae gap is nearly twice as large, and the RGB bump is 0.2 mag brighter (all implying lower metallicities), while the luminosity difference between the HB and subgiant branch (SGB) is 0.12 mag larger (implying older ages).

If we perform the same fits and comparisons with the 35 kpc population, we find that the populations at 21 and 35 kpc are distinct, but the changes with increasing radius are not monotonic. At $m_{F814W} = 27 \pm 0.5$ mag, the median RGB color of the 35 kpc population is only 0.004 mag bluer than that at 21 kpc (identical within the uncertainties). The RGB bump is not obvious in the 35 kpc fields; a slight overdensity of stars immediately below the red edge of the red clump may be due to the bump and clump merging, which would be consistent with a lower [Fe/H] than that in the 21 kpc field (where the RGB bump is bright but still distinct from the HB). All but 4 of the HB stars in the 35 kpc population fall in the red clump, whereas one would expect twice as many blue HB stars if the fraction of such stars exceeded that in the 21 kpc population. Although HB morphology tends to become bluer at decreas-

ing [Fe/H], several other parameters can affect the HB morphology; e.g., a younger age could compensate for a lower [Fe/H] to put more stars in the red clump. Comparing the luminosity functions of each field, the luminosity difference between the HB and SGB is ∼0.06 mag smaller in the 35 kpc fields than in the 21 kpc field, implying a somewhat younger age at 35 kpc. However, all of these visual inspections are hampered by the small number statistics in the 35 kpc fields.

Next we turn to quantitative fitting of the 35 kpc CMD, using the Starfish code of Harris & Zaritsky (2001), following the methodology of Brown et al. (2006). As done previously, we fit the lower RGB, SGB, and upper main sequence: $26.5 \leq m_{F814W} \leq 30$ mag and $-0.9 \leq m_{F606W} - m_{F814W} \leq -0.1$ mag (but excluding a 0.1×0.2 mag region at the blue HB); the fit thus avoids parts of the CMD with poor statistics, high foreground contamination, and poorly-understood dependence on age and [Fe/H]. The isochrone library comes from VandenBerg et al. (2006), transformed into the ACS bandpasses using the calibration of Brown et al. (2005). The age and metallicity distributions in these fits are shown in the bottom panels of Figure 2. From the weights in Figures 2h and 2i, we find that the <[Fe/H]> is 0.1 dex lower and the <age> is 0.5 Gyr younger in the 35 kpc field, compared to the 21 kpc field.

The 35 kpc population is inconsistent with a population that is ancient and coeval; a third of the stars in the best-fit model are younger than 10 Gyr. If we exclude such stars from the fits, the result is ruled out at 8σ (where σ is evaluated from repeated draws on the best-fit model), but the exclusion of stars younger than 6 Gyr is only ruled out at 2σ. A fit excluding super-solar metallicities is within 1σ of the best fit. Attempts to fit the 21 kpc and 35 kpc populations with the same star formation history imply they are distinct at more than 3σ. This is not due to small-number statistics in the 35 kpc field. If we fit 100 random draws of 8500 stars from the 21 kpc CMD, in 95% of the Monte Carlo runs the <age> is within 0.27 Gyr and the <[Fe/H]> is within 0.07 dex of the values in the best fit to the full 21 kpc CMD. If the best-fit models at 21 and 35 kpc are normalized to the same stellar mass, only 44% of that mass occupies the same age and [Fe/H] space.

4. SUMMARY AND DISCUSSION

We have measured the star formation history in three regions of the M31 spheroid, spanning a large range in distance on the minor axis (11 kpc, 21 kpc, and 35 kpc from the nucleus). The [Fe/H] decreases monotonically with increasing radius, with mean values of -0.65, -0.87, and -0.98, respectively. However, the age does not monotonically increase with increasing radius, having mean values of 9.68, 10.98, and

10.45 Gyr, respectively.

In their investigations of a metallicity gradient in the spheroid, Koch et al. (2007) find that <[Fe/H]> falls more rapidly with radius than Kalirai et al. (2006). Although our <[Fe/H]> at 35 kpc is in good agreement with the trend of Kalirai et al. (2006) and nearly 0.5 dex higher than that of Koch et al. (2007), the latter study includes 15 stars in the vicinity of our ACS fields, and for these, the <[Fe/H]> agrees well with our value. If the Koch et al. (2007) trend is representative of the general gradient in the spheroid, it would imply the ACS fields are in a local region of systematically higher [Fe/H]. Note that our fit uses the lower RGB, which is less sensitive to [Fe/H] than the upper RGB (used by Kalirai et al. and Koch et al.), but it provides a larger RGB sample and avoids the need to screen foreground dwarf contamination.

Our fits to the populations in the inner spheroid, the transition zone, and the outer spheroid all require the presence of intermediate-age stars (age < 10 Gyr). Such populations are expected if the spheroid formed via hierarchical assembly. This picture is also supported by recent star-count maps (Ibata et al. 2007) that show several stream-like structures crossing the minor axis beyond a distance of 40 kpc from the nucleus; relative to the bright ridge of stars in their Stream D (the nearest of these streams), our fields fall ∼30′ (7 kpc) toward the interior, and may conceivably include debris from these streams. Indeed, Bullock & Johnston (2005) argue that spheroids form inside-out, and that substructure should be abundant in the outer regions of the spheroid. A classical halo that is ancient and metal poor, as might be expected from an early monolithic collapse, does not comprise a large fraction of the population at 35 kpc. If we arbitrarily define such an ancient metal-poor population to be at [Fe/H]< −1.5 and age≥ 12 Gyr (considered representative of the outer regions of the Milky Way halo), the fraction of such stars in our best-fit model is only ∼10%. Recent surveys (e.g., Ibata et al. 2007) imply it will be difficult to find a truly "clean" region of the spheroid that is not criss-crossed by the debris of mergers.

REFERENCES

Brown, T.M., et al. 2005, AJ, 130, 1693
Brown, T.M., et al. 2007, ApJ, 658, L95
Brown, T.M., Ferguson, H.C., Smith, E., Kimble, R.A., Sweigart, A.V., Renzini, A., Rich, R.M., & VandenBerg, D.A. 2003, ApJ, 592, L17
Brown, T.M., Smith, E., Ferguson, H.C., Rich, R.M., Guhathakurta, P., Renzini, A., Sweigart, A.V., & Kimble, R.A. 2006, ApJ, 652, 323
Bullock, J.S., & Johnston, K.V. 2005, ApJ, 635, 921
Fardal, M.A., Guhathakurta, P., Babul, A., & McConnachie, A.W. 2007, MNRAS, 380, 15
Ferguson, A.M.N., Irwin, M.J., Ibata, R.A., Lewis, G.F., & Tanvir, N.R. 2002, AJ, 124, 1452
Flynn, C., Holmberg, J., Portinari, L., Fuchs, B., & Jahreiss, H. 2006, MNRAS, 372, 1149
Freedman, W.L., & Madore, B.F. 1990, ApJ, 365, 186
Fruchter, A.S., & Hook, R.N. 2002, PASP, 114, 144
Gilbert, K.M., et al. 2006, ApJ, 652, 1188
Gilbert, K.M., et al. 2007, ApJ, 669, 245
Guhathakurta, P., et al. 2006, AJ, 131, 2497

Guhathakurta, P., et al. 2005, arXiv preprint (astro-ph/0502366)
Hammer, F., Puech, M., Chemin, L., Flores, H., & Lehnert, M.D. 2007, ApJ, 662, 322
Harris, J., & Zaritsky, D. 2001, ApJS, 136, 25
Ibata, R., Irwin, M., Lewis, G., Ferguson, A.M.N., & Tanvir, N. 2001, Nature, 412, 49
Ibata, R., Martin, N.F., Irwin, M., Chapman, S., Ferguson, A.M.N., Lewis, G.F., & McConnachie, A.W. 2007, ApJ, 671, 1591
Irwin, M.J., Ferguson, A.M.N., Ibata, R.A., Lewis, G.F., & Tanvir, N.R. 2005, 628, L108
Kalirai, J.S., et al. 2006, ApJ, 648, 389
Koch, A., et al. 2007, ApJ, submitted, astro-ph/0711.458
Mould, J., & Kristian, J. 1986, ApJ, 305, 591
Pritchet, C.J., & van den Bergh, S. 1994, AJ, 107, 1730
Schlegel, D.J., Finkbeiner, D.P., & Davis, M. 1998, ApJ, 500, 525
Stetson, P. 1987, PASP, 99, 191
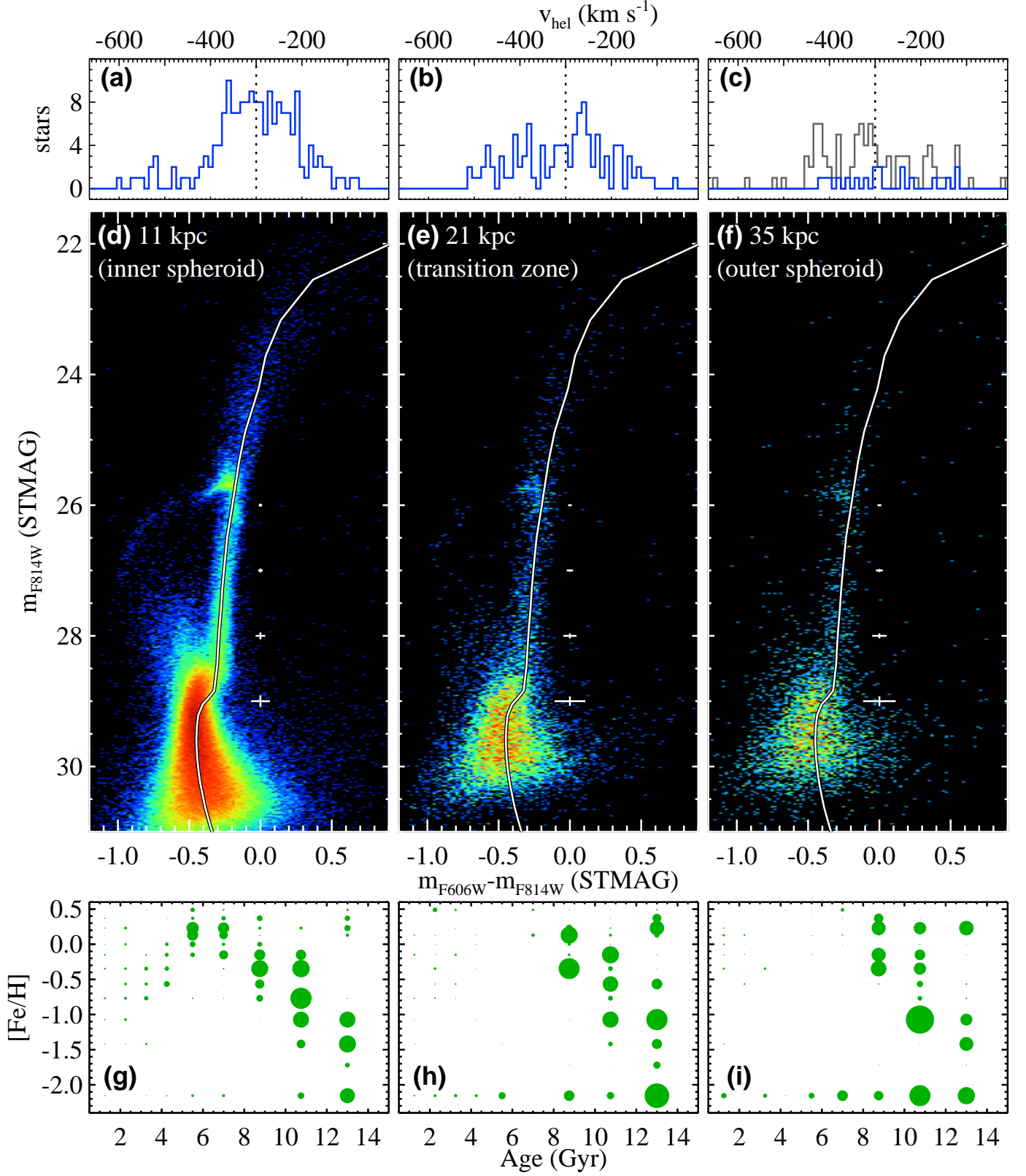VandenBerg, D.A., Bergbusch, P.A., & Dowler, P.D. 2006, ApJS, 162, 375

FIG. 2.— *(a–c)* Velocities for RGB stars within 9′ of our 11 kpc field, 14′ of our 21 kpc field, and 17′ of our 35 kpc fields (*blue histograms*); these samples are taken from survey regions that include and surround our ACS fields. The velocities in each region exhibit a broad distribution near the M31 systemic velocity (*dashed line*). To better demonstrate the broad (i.e., hot) distribution of velocities in the 35 kpc sample, we also show a dataset (*grey histogram*) that includes a region ∼30′ to the West of our 35 kpc field; Gilbert et al. (2007) find no significant cold component in this region. *(d–f)* CMDs for the populations at 11 kpc, 21 kpc, and 35 kpc. The ridge line of 47 Tuc (*white curve*; Brown et al. 2005), shifted to the M31 distance of 770 kpc (Freedman & Madore 1991) and reddening of $E(B-V) = 0.08$ mag (Schlegel et al. 1998) is shown for reference. *(g–i)* The best-fit star formation histories for the populations at 11 kpc, 21 kpc, and 35 kpc, from StarFish. The area of each filled circle is proportional to the number of stars at that age and metallicity. The populations in all three fields exhibit broad ranges of metallicity and age, but the population at 11 kpc includes far more stars younger than 8 Gyr (due at least in part to debris from the GSS).